Inhibition of EV71 replication by L3HYPDH, a newly identified interferon-stimulated gene product

Jian Liu,[a,b]* Luogen Liu,[a,b]* Shinuan Zeng,[a,b] Xiaobin Meng,[c] Nanfeng Lei,[c] Hai Yang,[c] Runcai Li,[a,b] Xuemin Guo[a,b]#

[a] *Institute of Human Virology, Zhongshan School of Medicine, Sun Yat-Sen University, Guangzhou Guangdong, China*

[2] *Key Laboratory of Tropical Disease Control (Sun Yat-Sen University), Ministry of Education, Guangzhou, Guangdong, China*

[3] *Meizhou People's Hospital, Meizhou, Guangdong, China*

Running Title: Activity and mechanism of L3HYPDH against EV71

#Address correspondence to Xuemin Guo, email: xmguo2005@yahoo.com

*Jian Liu and Luogen Liu contributed equally to this work.

Keywords: Interferon-stimulated gene, Enterovirus 71, L3HYPDH, Antiviral activity

Word counts for the abstract: 150

Word counts for the text: 4198

ABSTRACT

Up-regulation of interferon-stimulated genes (ISGs) is key to antiviral states mediated by interferon (IFN) but little is known about activity and underlying mechanisms of most ISGs against Enterovirus 71 (EV71). EV71 causes hand-foot-mouth disease in infants and occasionally severe neurological symptoms. Here we report that the product of *L3HYPDH*, a newly identified ISG, inhibits the replication of EV71. This anti-EV71 activity was mapped to the C-terminal 60 amino acids region as well as the N-terminal region spanning from amino acid position 61 to 120 of L3HYPDH protein. L3HYPDH was shown to interfere with EV71 propagation at the RNA replication and protein translation levels. Specifically, L3HYPDH impairs translation mediated by the EV71 international ribosome entry site (IRES) but not by the HCV IRES, and this activity is conferred by the C-terminal region of L3HYPDH. Thus, L3HYPDH has antiviral activity against EV71, suggesting a potential mechanism for broad-spectrum antiviral effects of IFN.

IMPORTANCE

Human EV71 can cause hand-foot-mouth disease (HFMD) and even death; however, no effective anti-EV71 treatment is available. Although EV71 suppresses induction of IFN and activation of IFN signaling pathways, type I IFN treatment can enhance the anti-EV71 state. IFN-stimulated genes (ISGs) are critical for innate immune defenses; however, the antiviral activities of many ISGs are not known. EV71 is seldom used for ISGs studies. So understanding the mechanism by which ISGs exert activity against EV71 will help to better understand IFN-triggered antiviral activity and provide new strategies to treat enterovirus infection. L3HYPDH is a newly identified ISG. We report here that L3HYPDH significantly inhibits EV71 replication by repressing RNA replication and protein translation, which suggests a mechanism underlying type I IFN against EV71. This would assist with the development of novel therapeutics to treat HFMD.

INTRODUCTION

Hand-foot-mouth disease (HFMD) is a common viral disease in infants and children across the Asian-Pacific region, characterized by fever, rash, and occasionally severe neurological symptoms (1, 2). Enterovirus 71 (EV71) is a major causative agent of HFMD. Different from many other viruses, EV71 suppresses induction of type I interferons (IFNs) and activation of IFN signaling pathways, and consequently, inhibits host anti-viral defenses (3-5). Nonetheless, EV71-infected cells still respond to type I IFN treatment and display an enhanced antiviral state. For example, *in vitro* studies showed that some type I IFNs, including IFN-α4, IFN-α6, IFN-α14 and IFN-α16, significantly reduced cytopathic effect (CPE) induced by EV71 infection (6). An IFN-α2b aerosol therapy has been used topically to treat HFMD (7). However, how IFNs suppress EV71 infection is not clear.

IFN-mediated antiviral mechanisms are diverse and complicated. Up-regulation of IFN-stimulated genes (ISGs) has shown to be critical to innate immune defenses against invading pathogens, so studies are underway to assess their functions and underlying mechanisms for developing future antiviral therapies. ISGs are abundant and different cells respond variously to different types of IFNs and the stimulation duration, resulting in diverse ISG expression patterns (8-10). Data of several systematic detections for antiviral activity suggest that different sets of ISGs target different viruses in unique ways, and antiviral roles may be broad or specific, strong or weak (11, 12). However, EV71 is seldom used for characterizing antiviral activity of ISGs, including well-characterized classic ISGs.

EV71 is enterovirus of the *Picornaviridae* family. Its genomic RNA is about 7400 nt long, single and positive-stranded, and contains only one open reading frame (ORF) flanked with a 5'-untranslated region (5'-UTR) and a 3'-UTR (1). The 5'-UTR contains a cloverleaf structure and an internal ribosome entry site (IRES), responsible for viral RNA replication and translation, respectively (13). The life cycle of EV71 starts with attachment to the host cell surface by recognition of a specific receptor, followed by endocytosis and release of viral RNA into the cytoplasm (14). Then, EV71 IRES initiates viral translation by recruiting host proteins. Synthesized polyproteins are processed into structural and non-structural proteins by its own protease 2A and 3C. When viral proteins accumulate, viral protein 3CD binds to the cloverleaf structure of 5'UTR to stop viral protein synthesis and initiates viral RNA replication. Produced RNAs then direct viral protein synthesis in large quantities. With the assembly of viral RNAs and proteins into virions, the host cell lyses and progeny viruses are released for a new round of infection (15, 16).

Many ISGs are antiviral effectors but these represent a few existing ISGs, and more will be identified. Recently, 91 new ISGs were identified from human immune cell lines after treatment with the consensus interferon (17), but their antiviral activity is unclear. Using a fluorescent activated cell sorting-based strategy for screening, we identified several ISGs with anti-EV71 efficacy (data not shown). One of them is *C14orf149*, which was identified as a gene encoding a trans-3-hydroxy-L-proline dehydratase and then renamed *L3HYPDH* (18). Here, we report that this ISG product, L3HYPDH, possesses antiviral activity against EV71, and its mechanism of action

97 was investigated with a series of biochemical and genetic assays.

98

99 **MATERIALS AND METHODS**

100 **Plasmids construction**

101 pCAG-DsRed, a red fluorescent protein-expressing plasmid, has been described
102 previously (19). pWSK-EV71-GFP is an infectious EV71-GFP cDNA clone, with a
103 GFP-coding sequence inserted downstream of EV71 5'UTR and in frame fusion with
104 the downstream *VP4*, and expression of EV71-GFP is driven by a T7 promoter (20).
105 pcDNA3.1-T7RNP expresses T7 RNA polymerase. These plasmids were kindly
106 provided by Dr. Liguo Zhang at the Institute of Biophysics, Chinese Academy of
107 Sciences (IBP, CAS). A siRNA targeting the coding sequence of *L3HYPDH* from
108 position 791 to 811 was designed according to the recommendation of Sigma-Aldrich
109 (https://www.sigmaaldrich.com/catalog/genes) and named shRNA149. A pair of
110 complementary oligonucleotides
111 5'-GATCCCCCAGATGAACAGGTTGACAGAATTCAAGAGATTCTGTCAACC
112 TGTTCATCTGTTTTTA-3' (sense) and 5'-AGCTTAAAAACAGATGAACA
113 GGTTGACAGAATCTCTTGAATTCTGTCAACCTGTTCATCTGGGG-3'
114 (antisense) were synthesized with 5' ends being *Bgl*II and *Hind*III restriction site
115 overhangs. For each oligonucleotide, the target sequence was sense followed by
116 antisense orientations separated by a nine-nucleotide spacer. Oligonucleotides were
117 annealed and then cloned into the *Bgl*II and *Hind*III sites of pSUPER.retro.neo+gfp
118 (Oligoengine, herein abbreviated for pSUPER-GFP) to generate

pSUPER-GFP-shRNA149. *L3HYPDH* wild type (WT) and deletion mutants as indicated in Fig 3 were amplified with PCR using pLPCX-C14orf149 (17), kindly provided by Dr. Guangxia Gao at IBP, CAS, as the template. PCR products of *L3HYPDH* WT and deleted mutants were digested with *BamH*I & *Not*I and *Kpn*I & *Xba*I, respectively, and inserted into similarly digested pcDNA4-To/myc-His B (Invitrogen), resulting in pcDNA4-L3HYPDH, pcDNA4-L3HYPDHΔN1, pcDNA4-L3HYPDHΔN2, pcDNA4-L3HYPDHΔN3, pcDNA4-L3HYPDHΔC1, pcDNA4-L3HYPDHΔC2, and pcDNA4-L3HYPDHΔC3. psiCHECK2-M was a modified form of psiCHECK-2 (Promega) with deletion of the HSV-TK promoter (Fig 5A). Inverse PCR was performed with high-fidelity DNA polymerase Phusion (ThermoFisher) and a pair of back-to-back primers to amplify the whole plasmid except the HSV-TK promoter sequence. PCR products were self-ligated and resulted in psiCHECK2-M; meanwhile, a *Sal*I and a *Not*I sites within the back-to-back primers were introduced into the plasmid. EV71-5'UTR and HCV-5'UTR were amplified from pWSK-EV71-GFP and pNL4-3RL-HCV-FL (21) by PCR, respectively. After digestion with *Sal*I and *Not*I, the PCR products were linked into the similarly digested psiCHECK2-M and resulted in psiCHECK2-M-EV71-5'UTR and psiCHECK2-M-HCV-5'UTR. All primers used are listed in Table S1.

Cell culture and virus preparation

293A, 293A-SCARB2, RD, Vero, Hela, and A549 cells were cultured in DMEM (Gibco) supplemented with 10% fetal bovine serum (FBS, Gibco). 293A-SCARB2 (Kindly provided by Dr. Liguo Zhang at IBP, CAS), originated from a 293A cell line

and constitutively expresses the main EV71 receptor scavenger receptor class B member 2 (SCARB2). To generate the cell line constitutively expressing tagged L3HYPDH, 293A-SCARB2 cells were transfected with pcDNA4-L3HYPDH as described below and selected with Zeocin (200 μg/ml). Resistant colonies were individually expanded and detected by Western blot. One positive clone was chosen and named 293A-SCARB2-L3HYPDH. This process was applied to the empty vector and resulted in control cell 293A-SCARB2-Ctrl.

EV71-MZ (GenBank accession no. KY582572), isolated from the throat swab of an ICU patient at Meizhou People's Hospital in 2014, was amplified by successive passages in RD cells until apparent CPE appeared. EV71-GFP was generated by co-transfecting pWSK-EV71-GFP and pcDNA3.1-T7RNAP into 293A-SCARB2 cells as described previously (20). Viral supernatants were titrated using a plague assay, aliquoted, and then used for infection.

Transfection and infection

Depending on the experiments, cells were seeded into a 24-well or 6-well plate or 10 cm dish and were grown to approximately 80% confluence prior to transfection or infection. All plasmid and RNA transfections were carried out by using Lipofectamine TM 2000 (Life Technology) according to the manufacturer's instructions. After incubation for the indicated time, cells were treated as required.

Viral infection was performed by incubating cells with EV71-GFP or EV71-MZ at a different multiplicity of infection (MOI) for 1 h, with shaking every 15 min, and then the unbound viruses were aspirated. Cells were washed with PBS, added fresh

163 medium and incubated for specific time, followed by FACS assay, RT-qPCR
164 measurement, or supernatant titration.

165 **Plaque assay**

166 The plaque assay was performed as described previously (22). Briefly, RD cells
167 were incubated with viral supernatants undiluted or diluted in 10-fold series for 1 h.
168 Subsequently, the supernatants were aspirated, and cells were covered with DMEM
169 containing 1% methylcellulose (Sigma-Aldrich) and 2% FBS. After incubation for 4
170 days, cells were fixed with 4% paraformaldehyde (Sigma-Aldrich) and stained with
171 0.1% crystal violet. Plaques were then quantified via visual scoring.

172 **Fluorescent activated cell sorting (FACS) assay**

173 To measure GFP production from EV71-GFP, 1×10^6 infected cells were collected
174 and fixed in 4% paraformaldehyde for 15 min. After washing three times with PBS,
175 cells were resuspended in 0.5 ml of PBS for flow cytometry (LSRFortessa, BD). To
176 assess effects of *L3HYPDH* knockdown by RNAi, the cells were transfected with
177 pSUPER-GFP-shRNA149 or pSUPER-GFP. After incubation for the indicated time,
178 the cells were harvested and washed with PBS. GFP-positive cells were obtained
179 through FACS, and then lysed for Western blot or seeded into a 24-well plate for
180 EV71-GFP infection or reporter plasmid transfection as required.

181 **IFN stimulation**

182 Cells were treated with 1000 IU/ml of recombinant human IFN-α2b (Prospec)
183 for different time, and then total RNAs were isolated and used to measure specific
184 mRNA abundance by RT-qPCR.

185 ***In vitro* transcription of EV71-GFP and microscope assay of GFP**

186 pWSK-EV71-GFP was linearized *Xba*I and EV71-GFP RNAs were transcribed
187 using the T7 RiboMax kit (Promega). After transfection into
188 293A-SCARB2-L3HYPDH and 293A-SCARB2-Ctrl cells, the GFP signal was
189 observed under a fluorescence microscope (System Microscope BX63, Olympus) at
190 the indicated times; total RNAs were isolated for RT-qPCR assay.

191 **RNA isolation and RT-qPCR**

192 Total RNAs were isolated from cells using TRI Reagent (Sigma-Aldrich)
193 according to the manufacturer's instructions. RT-qPCR was carried out as described
194 previously (23) to measure target mRNA. Briefly, RNAs were treated with DNase
195 using an RQ1 RNase-Free DNase Kit (Promega); cDNAs were synthesized using
196 PrimeScript RT reagent Kit (Takara, Dalian) and then diluted and subjected to
197 quantitative PCR using TransStart Green qPCR SuperMix (TransGen Biotch) in a
198 CFX96 Touch Real-Time PCR Detection System (Bio-Rad). Primers used appear in
199 Table S1.

200 **Immunofluorescence assay (IFA)**

201 Subcellular localization of L3HYPDH proteins and the attachment and
202 endocytosis of EV71 virions were detected using IFA as described previously (24)
203 with some modifications. Briefly, 293A-SCARB2-L3HYPDH and
204 293A-SCARB2-Crtl were individually seeded onto a coverslip. Polyclonal antibody
205 (PAb) specific to c-myc (Sigma-Aldrich, 1:100) and Alexa Fluor 555-labeled
206 anti-rabbit IgG (ThermoFisher, 1:100) were used as primary and secondary antibody,

207 respectively, to localize the subcellular distribution of the tagged L3HYPDH proteins.
208 Similarly, 293A-SCARB2-L3HYPDH and 293A-SCARB2-Crtl cells were infected
209 with EV71-MZ (MOI, 100) at 4°C for 1 h to allow viral attachment or incubated for
210 an additional 30 min at 37°C to allow viral endocytosis. The Anti-EV71 VP2
211 monoclonal antibody (MAb) (Millipore, 1:50) and Alex flour 555-labeled anti-mouse
212 IgG (ThermoFisher, 1:100) were used as primary and secondary antibody, respectively,
213 to visualize EV71 virions. Nuclei were stained with DAPI (Roche). Fluorescent
214 images of cells were captured using a Zeiss LSM780 META confocal imaging system.

215 **Western blot**

216 Western blot was performed as described previously (24) with some
217 modifications. Briefly, 48 h after transfection, the cells were lysed with SDS-lysis
218 buffer (30 mM SDS, 50 mM pH 6.8 Tris-HCL, 100 mM DTT and 20 mg/L
219 bromophenol blue) directly and proteins were isolated with 10% SDS-PAGE. The
220 membrane was probed with anti-6×His MAb (Abcam) and anti-GAPDH PAb
221 (Sangon), followed by incubation with HRP-conjugated anti-mouse IgG and
222 anti-rabbit IgG (Santa Cruz Biotechology), respectively. Proteins were visualized with
223 ECL.

224 **Luciferase activity assay**

225 Cell lysate was prepared by using passive lysis buffer (Promega). Firefly and
226 *renilla* luciferase activities were measured using a Dual Luciferase Assay kit
227 (Promega) according to the manufacturer's instructions.

228 **Statistical analysis**

All the experiments involving counting or calculation were performed independently at least three times and data are means ± standard deviation (SD). A Student's two-tailed *t* test was used for statistical analysis by using GraphPad Prism 6.1 (GraphPad 6 Software, San Diego, CA). $P< 0.05$ was considered statistically significant.

RESULTS

Over-expression of L3HYPDH inhibits EV71-GFP replication

The activity of L3HYPDH against EV71 was detected in 293A-SCARB2 cells using a FACS-based assay (Fig 1A). 293A-SCARB2 cells were used to facilitate EV71 infection. After co-transfection with pCAG-DsRed and pcDNA4-L3HYPDH at a ratio of 1:3, the cells were infected with EV71-GFP. All DsRed-expressing cells were assumed to express L3HYPDH, and viral replication in the DsRed-positive populations was quantified by FACS assay of GFP at 18 h post infection (Fig 1B). Cells overexpressing L3HYPDH expressed approximately 90% less GFP than control cells (Fig 1C). This result indicated that over-expression of exogenous L3HYPDH inhibits the expression of GFP, suggesting potential antiviral action against EV71 replication.

Expression of endogenous L3HYPDH suppresses EV71 replication

The expression of endogenous *L3HYPDH* and its response to IFN-α2b treatment were examined in different cell lines using RT-qPCR. Total RNAs were isolated from 293A, 293A-SCARB2, Vero, A549, RD, and Hela cells in the absence or presence of IFN-α2b for different times as indicated (Fig 2A, 2B). RT-qPCR assay showed that

the basal mRNA level of L3HYPDH was slightly higher in 293A, 293A-SCARB2 and Vero cells than in RD and A549, and the lowest in Hela cells (Fig 2A). Upon exposure to IFN-α2b, the level of L3HYPDH mRNA was up-regulated and peaked at about 18 h in 293A, 293A-SCARB2 and A549 and at about 12 h in Vero cells. Peak levels were 3 to 5 times higher than the basal level (Fig 2B). In contrast, the mRNA level changed little in Hela cells and even decreased a little in RD cells (Fig 2B). These results indicate that IFN-α2b stimulates the expression of L3HYPDH. However, the expression of L3HYPDH and its response to IFN-α2b differ in different cells, which is common for ISGs.

A shRNA specific to L3HYPDH, designated as shRNA149, was designed and transcribed from pSuper-GFP-shRNA149. Its knockdown efficiency was detected in 293A-SCARB2 cells by co-transfecting pcDNA4-L3HYPDH together with pSUPER-GFP-shRNA149 or with pSUPER-GFP as a control. Western blot analysis showed that the tagged L3HYPDH protein level decreased dramatically in the presence of shRNA149 (Fig 2C). To determine if the endogenous L3HYPDH could suppress EV71 replication, 293A-SCARB2 cells were transfected with pSUPER-GFP-shRNA149, and the GFP-positive cells were sorted by FACS, followed by EV71-MZ infection. RT-qPCR assay revealed that shRNA149 reduced L3HYPDH mRNA level by more than 80% (Fig 2D) and increased EV71 mRNA level from 1 to 1.7 (Fig 2E), indicating that the expression of endogenous L3HYPDH impaired EV71 replication. In this way, L3HYPDH possesses antiviral activity and is involved in the inherent cellular suppression on EV71 replication.

Determination of the amino acid sequences essential for anti-EV71 activity of

L3HYPDH

The region critical to L3HYPDH action against EV71 was mapped by serial deletions combination with the FACS-based assay. Three N-terminal and three C-terminal progressive deletion mutants of L3HYPDH are schematically shown in Fig 3 (middle panel), designated ΔN1, ΔN2, ΔN3, ΔC1, ΔC2, and ΔC3. Their coding sequences were cloned in fusion with a myc-6×His tag at the C-terminus as with L3HYPDH WT. The resulting plasmids were individually transfected into 293A-SCARB2 cells together with pCAG-DsRed followed by EV71-GFP infection as described in Fig 1A. Western blot showed that the protein levels of these truncated mutants were somewhat lower than that of WT, but still comparable (Fig 3, lower panel). FACS assay showed that L3HYPDHΔN2 lacking the amino acids from position 1 to 120 significantly impaired the antiviral activity in comparison with WT, while L3HYPDHΔN1 lacking the amino acids from position 1 to 60 only slightly weakened the antiviral activity. L3HYPDHΔC1 lacking the C-terminal 60 amino acids from 295 to 354 also weaken the antiviral activity somewhat, while further deletion did not heighten this impairment. These results indicate that the amino acid sequences from position 61 to 120 and from 295 to 354 are both required for the development of anti-EV71 activity of L3HYPDH.

EV71 replication is suppressed in the cell line 293A-SCARB2-L3HYPDH expressing L3HYPDH constitutively

To facilitate investigation of the antiviral mechanism, the cell line 293A-SCARB2- L3HYPDH expressing L3HYPDH constitutively and the corresponding control cell line 293A-SCARB2-Ctrl were generated. These two cell lines were infected with EV71-GFP at an MOI of 0.1. FACS assay showed that the

299 GFP production in 293A-SCARB2-L3HYPDH decreased to about 84% of control
300 levels (Fig 4A). Upon infection with EV71-MZ, a clinical isolate of EV71, there was
301 significantly less viral multiplication in 293A-SCARB2-L3HYPDH than in the
302 control cell (Fig 4B). IFA showed that L3HYPDH proteins were mainly located in the
303 cytoplasm (Fig 4C), consistent with its anti-EV71 action. Therefore, the cell
304 293A-SCARB2-L3HYPDH displays remarkable anti-EV71 activity due to the
305 over-expression of L3HYPDH, and thus can be exploited to uncover the underlying
306 antiviral mechanism.

307 **L3HYPDH interferes with the synthesis of viral RNA and proteins**

308 The effects of L3HYPDH on different life stages of EV71 replication were
309 examined in 293A-SCARB2-L3HYPDH cells. Based on the knowledge that EV71 is
310 only adsorbed on the cell surface and could not finish endocytosis at 4℃,
311 293A-SCARB2-L3HYPDH and the control cells were incubated with EV71-MZ for 1
312 h at 4℃ followed by IFA with the antibody specific to EV71 VP2. As shown in Fig
313 5A, massive number of virions distributed on the outer surfaces of both cell lines,
314 showing no difference in numbers, indicating that L3HYPDH could not interfere with
315 EV71 attachment. After attachment at 4℃, the viruses were further incubated with the
316 cells for an additional 30 min at 37℃ to complete endocytosis. IFA showed that many
317 viruses entered both cell lines, showing little difference (Fig 5B), indicating that
318 L3HYPDH had no effect on EV71 endocytosis. In this way, these results demonstrate
319 that L3HYPDH does not impede the viral attachment and endocytosis.

320 The effects of L3HYPDH on the synthesis of viral RNA and proteins were
321 investigated by monitoring changes in their levels over time.
322 293A-SCARB2-L3HYPDH and 293A-SCARB2-Ctrl cells were infected with

EV71-MZ. Total RNAs were isolated at different times post-infection and the viral RNA abundance was measured by RT-qPCR. The increase in EV71 RNA levels over time in 293A-SCARB2-L3HYPDH cells was much lower than in the control cells (Fig 5C). Due to the tight cross-talk between viral translation and viral RNA synthesis, these results suggested that L3HYPDH might inhibit the synthesis of viral RNA, proteins, or both. To further confirm this assumption, EV71-GFP RNAs were transfected into 293A-SCARB2- L3HYPDH and the control cell, and then the viral RNA and GFP proteins were measured and compared at different times after transfection. Microscope and RT-qPCR analyses showed that both the number of GFP-positive cells and the viral RNA level were much lower in 293A-SCARB2-L3HYPDH cells than in the control cells (Fig 5D, 5E). These results provide more evidence that L3HYPDH might suppress viral RNA replication, viral protein synthesis, or both.

L3HYPDH impairs the translation mediated by EV71-5'UTR

The repression of L3HYPDH on viral protein synthesis was investigated using a bicistronic reporter system. As shown in Fig 6A, psiCHECK-2-based reporter plasmids were constructed with the HSV-TK promoter deleted to generate the control (psiCHECK2-M) or replaced with EV71-5'UTR or HCV-5'UTR, which contains EV71 IRES or HCV IRES, respectively. pcDNA4-L3HYPDH or the empty vector was transfected into 293A cells together with one of the three reporter plasmids at a ratio of 3:1, and then the luciferase activity and mRNA level were measured after incubation for 48 h. For these reporters, the mRNA level ratio of *Fluc*/*Rluc* in L3HYPDH-overexpressed cells was equal to that in the empty vector-transfected cells as revealed by RT-qPCR (Fig 6B). However, the luciferase activity ratio (Fluc/Rluc) showed variability (Fig 6C). Whether L3HYPDH was over-expressed or not, the

Fluc/Rluc ratio of the control reporter was extremely low due to the absence of IRES; the ratio of the EV71-5'UTR-containing reporter reduced by 29% upon overexpression of L3HYPDH; while the ratio of the HCV-5'UTR-containing reporter changed little. We here proposed that L3HYPDH could specifically inhibit the reporter translation mediated by EV71 IRES. RNAi assay further provided evidence for this speculation. 293A-SCARB2-L3HYPDH cells were transfected with the shRNA149-expressing plasmid or the empty vector. Then the GFP-positive cells were isolated and transfected with the reporter plasmids. Compared to the control cells, the Fluc/Rluc ratio of the EV71-5'UTR-containing reporter in 293A-SCARB2-L3HYPDH cells increased moderately upon L3HYPDH knockdown (Fig 6D).

Given that the amino acid sequence from position 61 to 120 and the C-terminal 60 amino acids together contribute to anti-EV71 activity, we examined whether these sequences were involved in the action of inhibiting the EV71 IRES-mediated translation. 293A cells were transfected with the plasmids expressing L3HYPDH WT or deletion mutants together with the EV71-5'UTR-containing bicistronic reporter plasmids. Reporter assay revealed that, compared to the empty vector, the expression of WT, ΔN1, ΔN2 and ΔN3 reduced the Fluc/Rluc ratio by approximately 25% in 293A cells, consisting with the result shown above; while the expression of ΔC1, ΔC2, and ΔC3 had little effect on the ratio by comparison with control cells (Fig 6E). In combination with the results shown in Fig 3, these data indicate that the C-terminal sequence containing 60 amino acids from 295 to 354 is required for L3HYPDH to inhibit EV71-IRES-mediated translation.

Altogether, these results indicate that L3HYPDH can specifically impair the translation initiated by EV71-5'UTR, and the C-terminal region is responsible for this

373 inhibiting activity.

374

375 **DISCUSSION**

376 In this work, we report that the recently identified ISG product L3HYPDH has
377 antiviral activity against EV71 according to RNAi knockdown and over-expression
378 experiments. Over-expression of L3HYPDH repressed GFP production of EV71-GFP
379 (Fig 1B, 4B) and caused significant inhibition of propagation of the clinical isolate
380 EV71-MZ (Fig 4C). *L3HYPDH* knockdown increased EV71 mRNA in 293A-CARB2
381 cells (Fig 2E), highlighting that this gene is an important ISG with antiviral activity.
382 Additionally, our data showed that IFN-α2b treatment was less effective against EV71
383 in cell culture when expression of L3HYPDH was depressed by RNAi (Fig S1).
384 Therefore, L3HYPDH is key to antiviral activity of IFN-α2b against EV71. The
385 potential activity of L3HYPDH against other viruses is not known. Given that
386 different viruses are usually targeted by unique sets of ISGs (11), an extensive
387 investigation on L3HYPDH will help to further elucidate the mechanism of
388 IFN-mediated innate immunity against invading viruses.

389 Our data show that L3HYPDH may interfere with EV71 replication at post-entry
390 stage (Fig 4). Bicistronic reporter assays confirmed that expression of L3HYPDH
391 inhibited translation initiated by EV71 IRES (Fig 6B), however, the reporter protein
392 was less reduced than EV71 RNA and virus-carrying GFP production during the first
393 round of infection (Fig 1B, 4A, 5C-E). These inconsistences suggest that L3HYPDH
394 hampers EV71 replication at steps other than translation. Although inhibition of viral

RNA replication is likely, other potential effects on viral RNA stability, viral assembly and viral release cannot be excluded. Therefore, L3HYPDH inhibits EV71 replication at least at two levels, and these data are in agreement with previous studies indicating that many ISGs block viral replication at multiple stages of the viral life cycle (25-27). Considering that a range of proteins are involved in the viral RNA replication and translation process, we performed co-immunoprecipitation and tandem affinity purification combination mass spectrometry to screen for proteins interacting with L3HYPDH. Neither viral nor host proteins were identified (data not shown). These results suggest that the association of L3HYPDH proteins with other proteins should be transient or weak. L3HYPDH might also function by binding to the viral RNA directly; however, no known RNA-binding domains were predicted with online software (data not shown).

Viral translation is completely host cell-dependent. To maximize efficiency, different viruses evolved many strategies to facilitate selective translation of viral mRNAs over host transcripts (15, 28-30). Among these, the IRES-mediated translation initiation is necessary for picornavirus and hepacivirus to replicate (13, 31). Reporter assays showed that expression of L3HYPDH impaired initiation of translation mediated by EV71 IRES but not HCV IRES (Fig 6B, 6C). These two IRES differ in nucleotide length and structure as well as in host factors required for translation initiation and regulation (32). A potential target of L3HYPDH should be involved in EV71-5'UTR-mediated translation. Given that an ISG may interfere with different stages of different viral life cycles, whether L3HYPDH has the activity against HCV is unclear. Meanwhile, despite being present in all picornaviruses, IRES is diverse in length and structure and requires different host factors to function

(33-35). Whether L3HYPDH can inhibit other genuses of picornavirus by interfering with IRES-mediated translation is not clear is not clear, but this is worthy of study.

L3HYPDH is a trans-3-hydroxy-L-proline dehydratase, and specifically catalyzes the dehydration of dietary trans-3-hydroxy-L-proline and from degradation of proteins such as collagen IV that contain it. This dehydratase contains two active sites, a Cys residue at the 104 position and a Thr residue at the 273 position (18). Interestingly, the region required for anti-EV71 activity was mainly mapped to the amino acid sequence from position 61 to 120 of L3HYPDH protein (Fig 3), which contains the Cys104 active site. Whether this proline dehydratase activity is involved in the anti-EV71 activity is not known. L3HYPDH functions as an anti-EV71 effector. Understanding ISG products and antiviral spectra, as well as their mechanisms of action and biological function will help create novel therapeutics for HFMD.

ACKNOWLEDGEMENTS

This work was supported by the grants from Guangdong Innovative Research Team Program (2009010058), the National Key Program for Infectious Disease of China (2012ZX10001003), and Science and Technology Planning Project of Guangdong Province (A2016467 to X. Meng). We thank Dr. Liguo Zhang for providing the plasmids pCAG-DsRed, pWSK-EV71-GFP, pcDNA3.1-T7RNP and the cell line 293A-SCARB2. We also thank Dr. Guangxia Gao for providing the plasmids pLPCX-C14orf149 and pNL4-3RL-HCV-FL.

REFERENCES

1. **Brown BA, Oberste MS, Alexander JP, Jr., Kennett ML, Pallansch MA.** 1999. Molecular epidemiology and evolution of enterovirus 71 strains isolated from

1970 to 1998. J Virol **73:**9969-9975.

2. **Mcminn PC.** 2002. An overview of the evolution of enterovirus 71 and its clinical and public health significance. FEMS Microbiol Rev **26:**91-107.

3. **Lei X, Liu X, Ma Y, Sun Z, Yang Y, Jin Q, He B, Wang J.** 2010. The 3C Protein of Enterovirus 71 Inhibits Retinoid Acid-Inducible Gene I-Mediated Interferon Regulatory Factor 3 Activation and Type I Interferon Responses. J Virol **84:**8051-8061.

4. **Lei X, Sun Z, Liu X, Jin Q, He B, Wang J.** 2011. Cleavage of the adaptor protein TRIF by enterovirus 71 3C inhibits antiviral responses mediated by Toll-like receptor 3. J Virol **85:**8811-8818.

5. **Lu J, Yi L, Zhao J, Yu J, Chen Y, Lin MC, Kung HF, He ML.** 2012. Enterovirus 71 disrupts interferon signaling by reducing the level of interferon receptor 1. J Virol **86:**3767-3776.

6. **Yi L, He Y, Chen Y, Kung HF, He ML.** 2011. Potent inhibition of human enterovirus 71 replication by type I interferon subtypes. Antiviral Ther **16:**51-58.

7. **Lin H, Huang L, Zhou J, Lin K, Wang H, Xue X, Xia C.** 2016. Efficacy and safety of interferon-alpha2b spray in the treatment of hand, foot, and mouth disease: a multicenter, randomized, double-blind trial. Arch Virol **161:**3073-3080.

8. **De Veer MJ, Holko M, Frevel M, Walker E, Der S, Paranjape JM, Silverman RH, Williams BRG.** 2001. Functional classification of interferon-stimulated genes identified using microarrays. J Leukoc Biol **69:**912-920.

9. **Der SD, Zhou A, Williams BRG, Silverman RH.** 1998. Identification of genes

differentially regulated by interferon α, β, or γ using oligonucleotide arrays. Proc Natl Acad Sci U S A **95:**15623-15628.

10. **Liu SY, Sanchez DJ, Aliyari R, Lu S, Cheng G.** 2012. Systematic identification of type I and type II interferon-induced antiviral factors. Proc Natl Acad Sci U S A **109:**4239-4244.
11. **Schoggins JW, Rice CM.** 2011. Interferon-stimulated genes and their antiviral effector functions. Curr Opin Virol **1:**519-525.
12. **Schneider WM, Chevillotte MD, Rice CM.** 2014. Interferon-stimulated genes: a complex web of host defenses. Annu Rev Immunol **32:**513-545.
13. **Martínez-Salas E, Francisco-Velilla R, Fernandez-Chamorro J, Lozano G, Diaz-Toledano R.** 2015. Picornavirus IRES elements: RNA structure and host protein interactions. Virus Res **206:**62-73.
14. **Dang M, Wang X, Wang Q, Wang Y, Lin J, Sun Y, Li X, Zhang L, Lou Z, Wang J, Rao Z.** 2014. Molecular mechanism of SCARB2-mediated attachment and uncoating of EV71. Protein Cell **5:**692-703.
15. **Lin JY, Chen TC, Weng KF, Chang SC, Chen LL, Shih SR.** 2009. Viral and host proteins involved in picornavirus life cycle. J Biomed Sci **16:**103.
16. **Lei X, Cui S, Zhao Z, Wang J.** 2015. Etiology, pathogenesis, antivirals and vaccines of hand, foot, and mouth disease. Natl Sci Rev **2:**268-284.
17. **Zhang X, Yang W, Wang X, Zhang X, Tian H, Deng H, Zhang L, Gao G.** 2018. Identification of new type I interferon-stimulated genes and investigation of their involvement in IFN-beta activation. Protein Cell **1-9**.

18. **Visser WF, Verhoeven-Duif NM, de Koning TJ.** 2012. Identification of a human trans-3-hydroxy-L-proline dehydratase, the first characterized member of a novel family of proline racemase-like enzymes. J Biol Chem **287:**21654-21662.

19. **Matsuda T, Cepko CL.** 2004. Electroporation and RNA interference in the rodent retina in vivo and in vitro. Proc Natl Acad Sci U S A **101:**16-22.

20. **Zhang X, Yang P, Wang N, Zhang J, Li J, Guo H, Yin X, Rao Z, Wang X, Zhang L.** 2017. The binding of a monoclonal antibody to the apical region of SCARB2 blocks EV71 infection. Protein Cell **8:**590-600.

21. **Zhu Y, Wang X, Goff SP, Gao G.** 2012. Translational repression precedes and is required for ZAP-mediated mRNA decay. EMBO J **31:**4236-4246.

22. **Tang WF, Huang RT, Chien KY, Huang JY, Lau KS, Jheng JR, Chiu CH, Wu TY, Chen CY, Horng JT.** 2015. Host miR-197 plays a negative regulatory role in the enterovirus 71 infectious cycle by targeting the RAN protein. J Virol **90:**1424-1438.

23. **Zhou S, Chen X, Meng X, Zhang G, Wang J, Zhou D, Guo X.** 2015. "Roar" of blaNDM-1 and "silence" of blaOXA-58 co-exist in Acinetobacter pittii. Sci Rep **5:**8976.

24. **Li K, Zhou S, Guo Q, Chen X, Lai DH, Lun ZR, Guo X.** 2017. The eIF3 complex of Trypanosoma brucei: composition conservation does not imply the conservation of structural assembly and subunits function. RNA **23:**333-345.

25. **Pichlmair A, Lassnig C, Eberle CA, Gorna MW, Baumann CL, Burkard TR, Burckstummer T, Stefanovic A, Krieger S, Bennett KL, Rulicke T, Weber F,**

Colinge J, Muller M, Superti-Furga G. 2011. IFIT1 is an antiviral protein that recognizes 5'-triphosphate RNA. Nat Immunol **12:**624-630.

26. **Kato H, Takeuchi O, Sato S, Yoneyama M, Yamamoto M, Matsui K, Uematsu S, Jung A, Kawai T, Ishii KJ.** 2006. Differential roles of MDA5 and RIG-I helicases in the recognition of RNA viruses. Nature **441:**101-105.
27. **Haller O, Kochs G.** 2011. Human MxA protein: an interferon-induced dynamin-like GTPase with broad antiviral activity. J Interferon Cytokine Res **31:**79-81.
28. **Du H, Yin P, Yang X, Zhang L, Jin Q, Zhu G.** 2014. Enterovirus 71 2C Protein Inhibits NF-κB Activation by Binding to RelA(p65). Sci Rep **5:**14302.
29. **Sharma R, Raychaudhuri S, Dasgupta A.** 2004. Nuclear entry of poliovirus protease-polymerase precursor 3CD: implications for host cell transcription shut-off. Virology **320:**195-205.
30. **Weng KF, Li ML, Hung CT, Shih SR.** 2009. Enterovirus 71 3C Protease Cleaves a Novel Target CstF-64 and Inhibits Cellular Polyadenylation. PLoS Pathog **5:**e1000593.
31. **Honda M, Ping LH, Rijnbrand RC, Amphlett E, Clarke B, Rowlands D, Lemon SM.** 1996. Structural requirements for initiation of translation by internal ribosome entry within genome-length hepatitis C virus RNA. Virology **222:**31-42.
32. **Michael Gale J, Tan SL, Katze MG.** 2000. Translational Control of Viral Gene Expression in Eukaryotes. Microbiol Mol Biol Rev **64:**239-280.

532 33. **Gingras AC, Svitkin Y, Belsham GJ, Pause A, Sonenberg N.** 1996. Activation
533 of the Translational Suppressor 4E-BP1 Following Infection with
534 Encephalomyocarditis Virus and Poliovirus. Proc Natl Acad Sci U S A
535 **93:**5578-5583.
536 34. **Andreev DE, Fernandezmiragall O, Ramajo J, Dmitriev SE, Terenin IM,**
537 **Martinezsalas E, Shatsky IN.** 2007. Differential factor requirement to assemble
538 translation initiation complexes at the alternative start codons of foot-and-mouth
539 disease virus RNA. RNA **13:**1366-1374.
540 35. **Sweeney TR, Abaeva IS, Pestova TV, Hellen CU.** 2014. The mechanism of
541 translation initiation on Type 1 picornavirus IRESs. EMBO J **33:**76–92.
542
543

Figure Legends

Fig 1. FACS-based assay for antiviral activity of L3HYPDH against EV71-GFP replication. (A) Overview of the procedures detecting anti-EV71 activity of over-expressed L3HYPDH using FACS. (B) FACS plots of L3HYPDH inhibition of EV71-GFP in 293A-SCARB2 cells. Numerals represent percent of total cell counts. (C) GFP production, which was calculated by multiplying GFP and DsRed co-positive cell number by the mean value of GPF intensity. The value of the control cells transfected with empty vector was set as 100%. Results are represented as means ± SD of three independent experiments. *, $P< 0.05$.

Fig 2. Anti-EV71 activity of the endogenous L3HYPDH. (A) RT-qPCR assay of the endogenous *L3HYPDH* mRNA level in different cell lines, which was normalized to *GAPDH* mRNA level. (B) RT-qPCR assay of *L3HYPDH* expression with IFN-α2b (1000 IU/ml) treatment for indicated time in different cell lines. *L3HYPDH* mRNA level was normalized to that of GAPDH. The relative mRNA level from untreated cells (marked as 0 h) was set as 1. (C) Western blot of knockdown efficiency of shRNA149 targeting *L3HYPDH*. 293A-SCARB2 cells were transfected with pcDNA4-L3HYPDH together with shRNA149-expressing plasmid or control plasmid (Crtl) at a ratio of 1:3.The GFP-positive cells were sorted and then infected with EV71, followed by RT-qPCR analyses of *L3HYPDH* mRNA (D) and EV71 *2C* mRNA after depression of L3HYPDH expression. RT-qPCR data are means ± SD of three independent experiments. *, $P<0.05$.

Fig 3. Mapping amino acid sequence required for anti-EV71 activity of

L3HYPDH. Deletion mutants of L3HYPDH were schematically shown in the middle panel. Numbers indicate starting and ending amino acid. The plasmids expressing L3HYPDH wild type (WT) or truncated mutants were individually transfected into 293A-SCARB2 cells together with pCAG-DsREd at a ratio of 3:1, followed by EV71-GFP infection. Same performance was done the empty vector used as a control (Ctrl). L3HYPDH WT proteins or deletion mutants were analyzed by Western blot with anti-6×His MAb (lower panel). GFP production from EV71-GFP was detected using FACS and calculated as described in Fig1C. The value from control was set as 100%. Data are represented as mean ± SD of three independent experiments. *, $P<$ 0.05.

Fig 4. Evaluating antiviral activity of 293A-SCARB2- L3HYPDH cells. 293A-SCARB2-L3HYPDH and the control cell 293A-SCARB2-Ctrl were infected with EV71-GFP (MOI, 0.1). GFP production was detected using FACS (A) and calculated (B). Data are represented as mean ± SD of three independent experiments. *, $P<$ 0.05. (C) Time-viral yield assay. 293A-SCARB2-L3HYPDH and the control cell were individually infected with EV71-MZ (MOI, 2). The culture supernatants were harvested at different time points as indicated and titrated by plague assay. Data for each time point are means ± SD of three independent experiments. (D) Subcellular localization of tagged L3HYPDH proteins using IFA. Nuclear DNA was stained with DAPI.

Fig 5. Stage assays for unveiling the mechanism of L3HYPDH against EV71. Effect of L3HYPDH on attachment (A) and endocytosis (B) of EV71 was examined using IFA. 293A-SCRB2-L3HYPDH and 293A-SCARB2-Ctrl cells were infected

589 with EV71-MZ (MOI, 100). Nuclei were stained with DAPI. (C) Effect of L3HYPDH
590 on viral RNA measured with RT-qPCR. 293A-SCARB2-L3HYPDH and control cell
591 (Ctrl) were infected with EV71-MZ (MOI, 2). EV71 *2C* mRNA level was measured at
592 indicated times and normalized to that of *GAPDH*, with the relative level in control
593 cell at 2 h post infection set as 1. EV71-GFP RNAs were transfected into
594 293A-SCARB2-L3HYPDH and control cell (Ctrl). GFP signal and EV71 2C RNA
595 level at different times post transfection were examined by fluorescent microscope (D)
596 and RT-qPCR (E), respectively. All the RT-qPCR data are represented as means ± SD
597 of three independent experiments. *, $P<0.05$.

598 **Fig 6. Bicistronic reporter assay to measure the effect of L3HYPDH on EV71**
599 **IRES mediated translation.** (A) Schematic of bicistronic reporters. Rluc is translated
600 in a cap-dependent manner and Fluc in an IRES-dependent manner.
601 pcDNA4-L3HYPDH or empty vector was transfected into 293A cells together with
602 psiCHECK2-M, psiCHECK2-EV71-5'UTR, or psiCHECK2-HCV-5'UTR. Effects of
603 L3HYPDH on the reporter expression were estimated by RT-qPCR (B) and luciferase
604 activity assay (C). Fluc/Rluc ratio was calculated, with the relative value from the
605 cells transfected with empty vectors was set as 1. (D) RNAi assay of effect of
606 L3HYPDH on reporter expression mediated by IRES. pSUPER-GFP-shRNA149 or
607 pSUPER-GFP was transfected into 293A-SCARB2-L3HYPDH cell. The GFP
608 positive cells were transfected with psiCHECK2-M or psiCHECK2-M-EV71-5'UTR.
609 Luciferase activity was measured, with Fluc/Rluc ratio from cells co-transfected with
610 psiCHECK2-M and pSUPER-GFP set as 1. (E) Effect of L3HYPDH deletion on
611 reporter expression. The plasmids expressing L3HYPDH WT or deletion mutants
612 were individually transfected into 293A cells together with
613 psiCHECK2-EV71-5'UTR at a ratio of 3:1. Transfection with pcDNA4 was used as a

614 control (Ctrl). Luciferase activities were measured. Fluc/Rluc ratio was calculated,
615 with the relative value from the cells transfected with the empty vector set as 1. Data
616 are means ± SD of three independent experiments. *, $P< 0.05$.
617

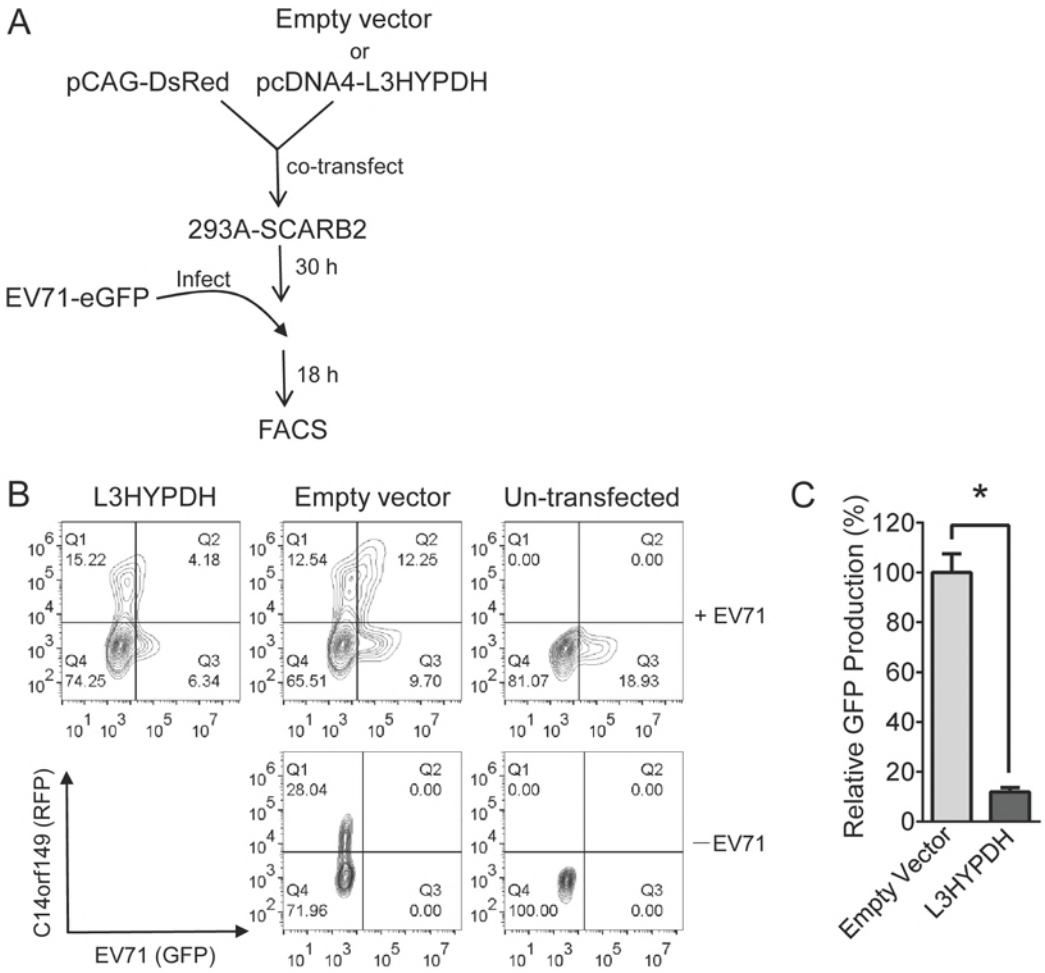

Figure 1

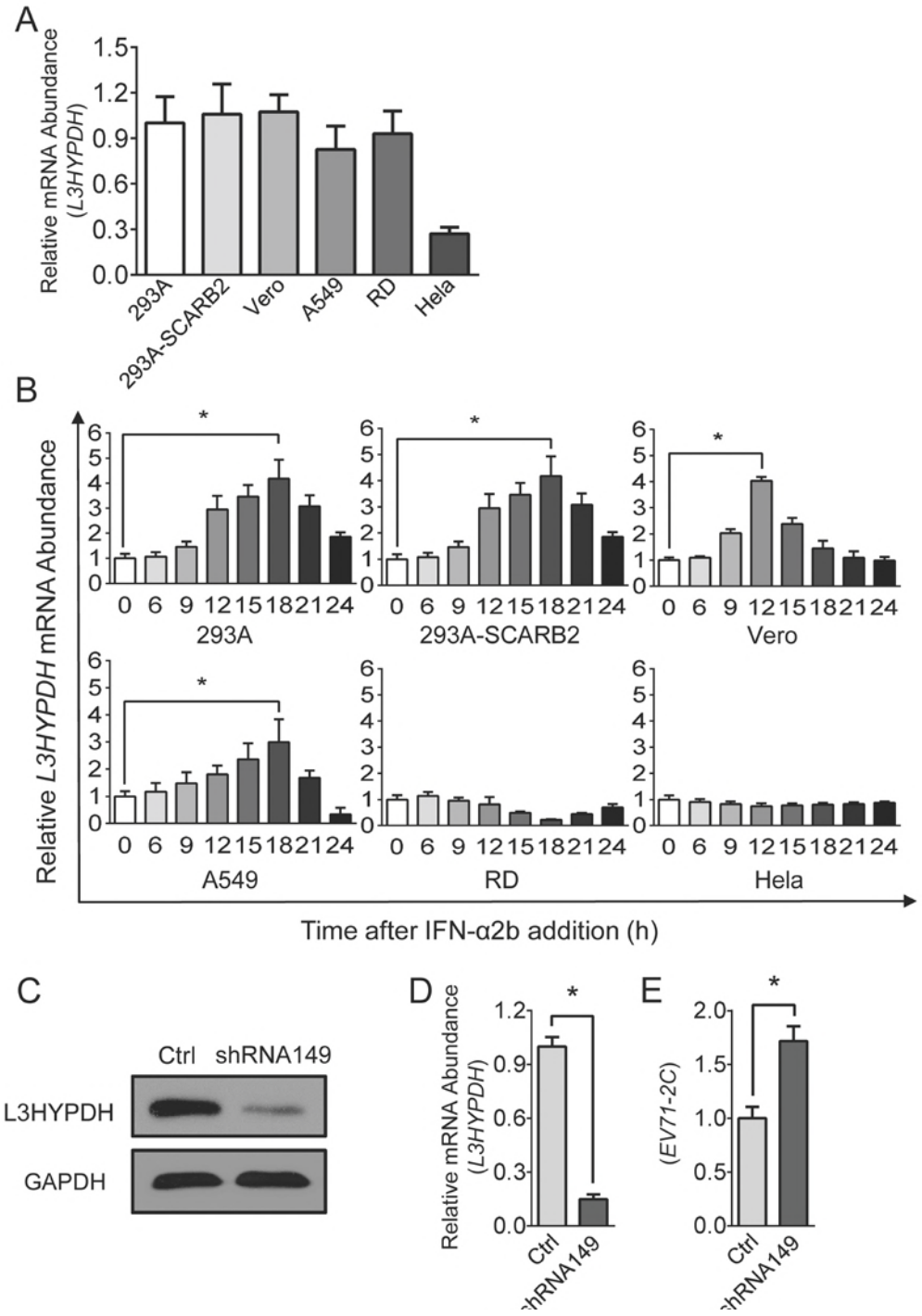

621

622

623 Figure 2

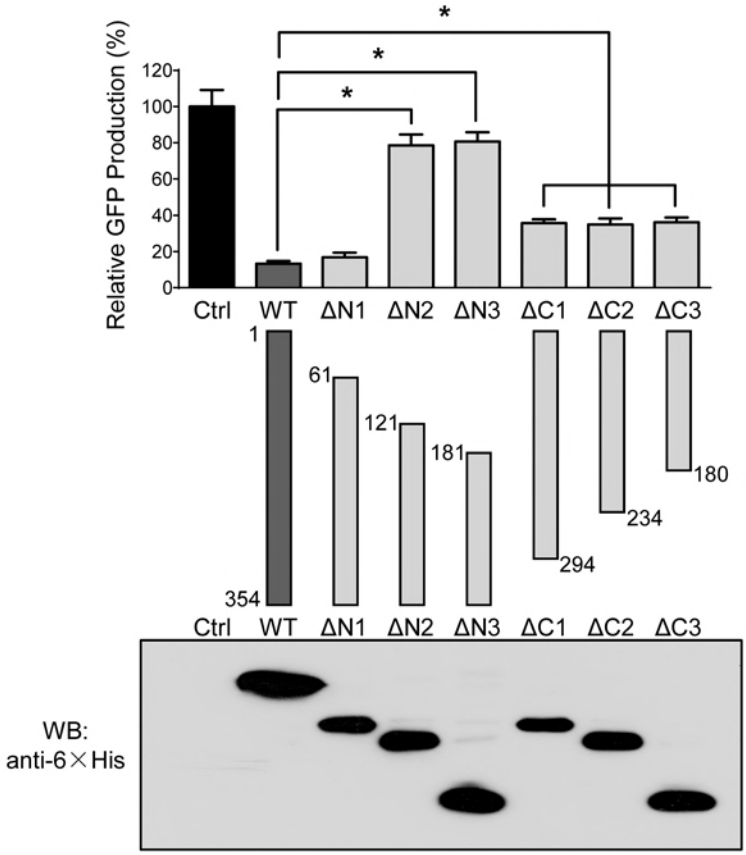

624

625

626 Figure 3

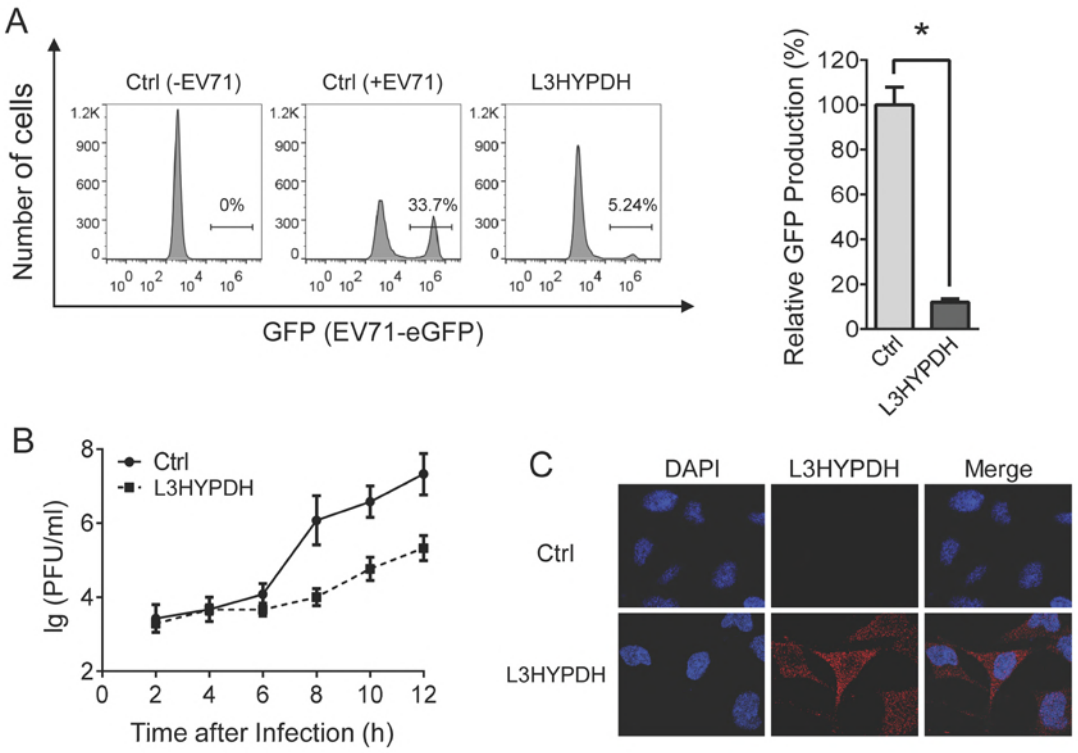

627

628

629 Figure 4

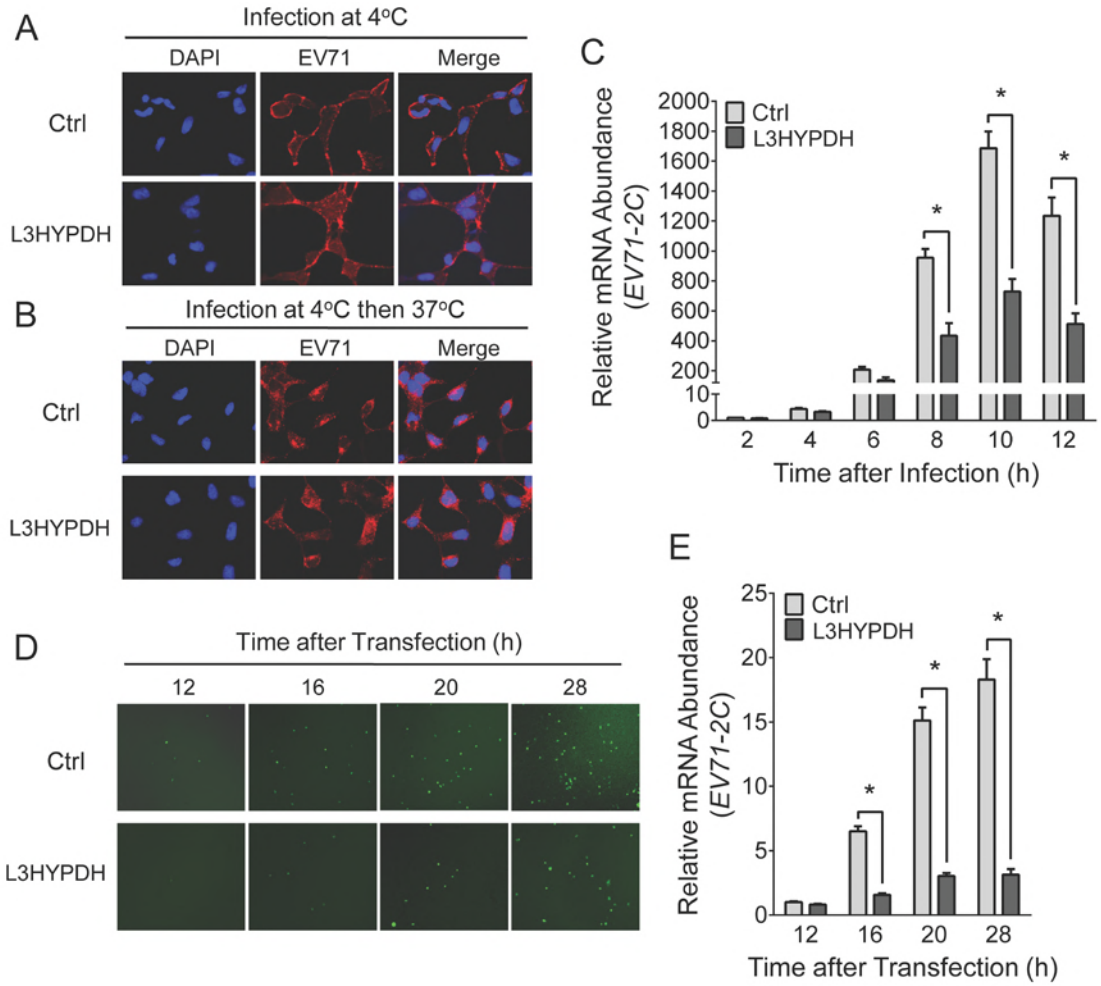

630

631

632 Figure 5

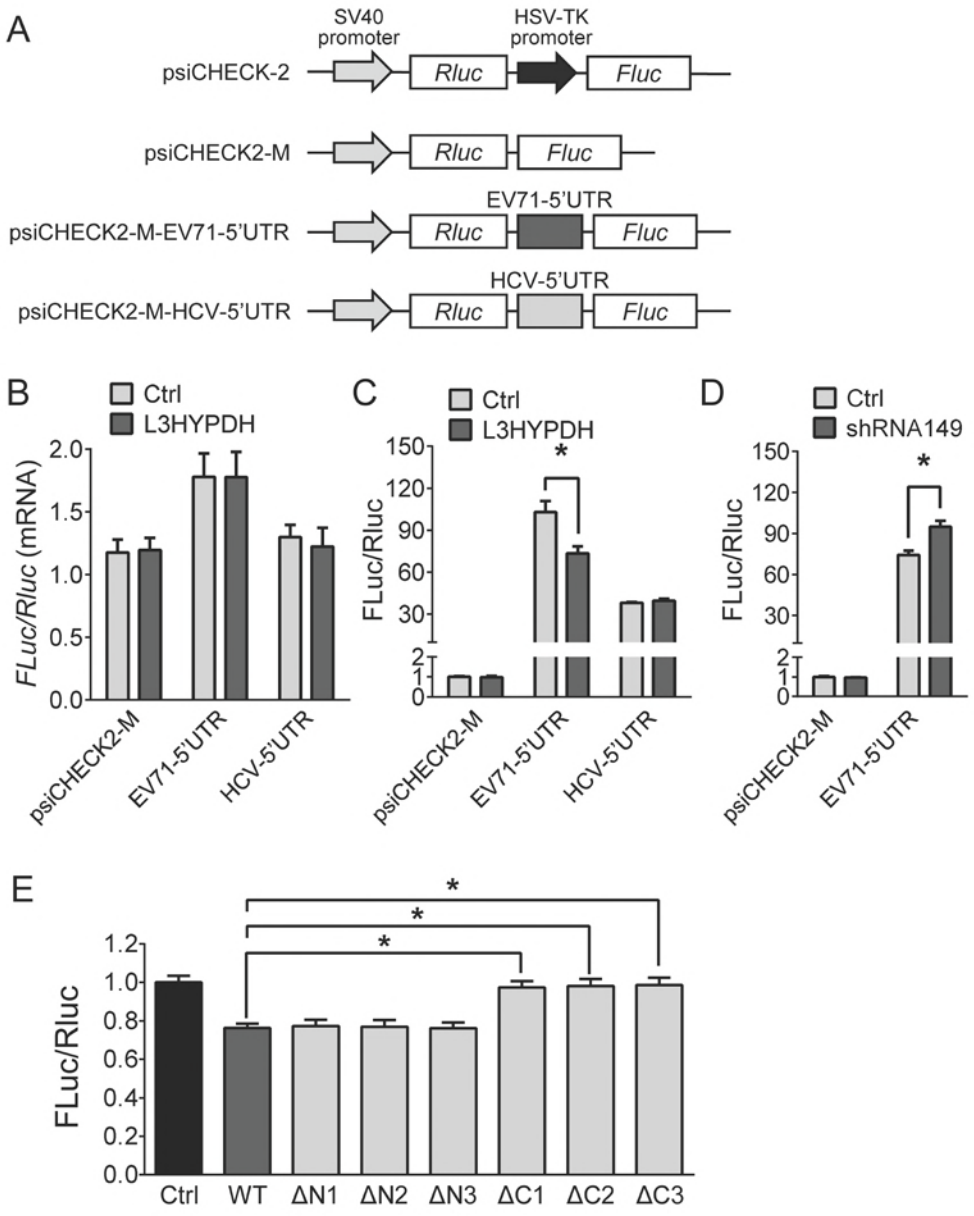

633

634

635 Figure 6

Table S1 Primers used in this study

Name	Sequence (5’-3’)	Target gene, usage
L3HYPDH-F	CGGGATCCGCCACCATGGAGAGCGC[a]	*L3HYPDH*
L3HYPDH-R	CACGCGGCCGCACTTGAGAAGAAATCCA	
L3HYPDH-N1-F	CACGGTACCATGGTGCGGCGACGGCTCA	L3HYPDHΔN1
L3HYPDH-N-R	CACTCTAGACTGCACTTGAGAAGAAAT	
L3HYPDH-N2-F	CACGGTACCATGGTGCCGGCGCCCCCTG	Pairing with L3HYPDH-N-R, L3HYPDHΔN2
L3HYPDH-N3-F	CACGGTACCATGGGAAAGGTGATGGTGG	Pairing with L3HYPDH-N-R, L3HYPDHΔN3
L3HYPDH-C-F	CACGGTACCATGGAGAGCGCGCTGG	L3HYPDHΔC1
L3HYPDH-C1-R	CACTCTAGACTCATCTGGTTCAGTTCC	
L3HYPDH-C2-R	CACTCTAGACTTTCACTATCAGGATGA	Pairing with L3HYPDH-C-F, L3HYPDHΔC2
L3HYPDH-C3-R	CACTCTAGACTATGTCCAGGAACATCC	Pairing with L3HYPDH-C-F, L3HYPDHΔC3
CHECK2-F	CACGCGGCCGCTCTAGGTTTAAA	Back-to-back primers, used for generating psiCHECK2-M
CHECK2-R	CACGTCGACATGGCCGATGCTAAGAACATTA	
EV71-5’UTR-F	CACGCGGCCGCTTAAAACAGCCTGTGG	EV71-5’UTR
EV71-5’UTR-R	CACGTCGACGTTTAGCTGTGTTAAGG	
HCV-5’UTR-F	CACGCGGCCGCGGCGACACTCCACCATAG	HCV-5’UTR
HCV-5’UTR-R	CACGTCGACGATGCACGGTCTACGA	
QL3HYPDH-F	AGGAGTGACAGCC CGAATTG	*L3HYPDH*, used for qPCR
QL3HYPDH-R	CACATTTCGCTTCCCTCACAG	
QEV71-2C-F	TGTATGTCTCATTATCAGGGG	EV71 *2C*, used for qPCR
QEV71-2C-R	CCACCTGTTGCTTGTAACCGT	
QRluc-F	ATAACTGGTCCGCAGTGGTG	*Rluc*, used for qPCR
QRluc-R	AGGCC GCGTTACCATGTAAA	

QFluc-F	AGCACTTCTTCATCGTGGACCG	*Fluc*, used for qPCR
QFluc-R	GGCAGCTCGCCGGCATCGTCGT	
H-QGAPDH-F	GAAGGTGAAGGTCGGAGT	Human *GAPDH*, used for qPCR[b]
H-QGAPDH-R	GAAGATGGTGATGGGATTTC	
Vero-QGAPDH-R	GAAGATGGTGATGGGGCTTC	Pairing with H-QGAPDH-F, Monkey *GAPDH*, used for qPCR of the RNA from Vero cells

[a] Restriction sites are underlined.

[b]The primers against human *GAPDH* have been described elsewhere (Ng *et al*., 2002. Clinical Chemistry). All other primers used for the PCR assays are designed using the Primer-BLAST tool (https://www.ncbi.nlm.nih.gov/tools/primer-blast/) or acquired from Primer Bank (https://pga.mgh.harvard.edu/primerbank/).

Knockdown of L3HYPDH impairs anti-EV71 efficacy of IFN-α2b

IFN-α2b treatment combination with RNAi assay were performed to further determine if the endogenous L3HYPDH could suppress EV71 replication, 293A-SCARB2 cells were transfected with pSUPER-GFP-shRNA149, and the GFP-positive cells were sorted by FACS and divided into two parts for IFN-α2b treatment and mock-treatment, followed by EV71-MZ infection. RT-qPCR assay revealed that the IFN treatment caused a triple increase of the endogenous *L3HYPDH* mRNA level (Figure S1A) and about 40% reduction in the EV71 RNA abundance in 293A-SCARB2 cells (Figure S1B), further validating the perspective that type I IFN is capable of inhibiting EV71 infection. When the expression of *L3HYPDH* was reduced by approximate 80% by RNAi, IFN-α2b treatment was less effective against EV71 replication and the viral RNA level increased from 0.6 to 0.78 (Figure S1A, S1B). Although the increase in viral yield was not significant, the results indicated that the *L3HYPDH* products play an irreplaceable role in the anti-EV71 action intrigued by IFN-α2b, suggesting *L3HYPDH* as an important ISG possessing antiviral activity.

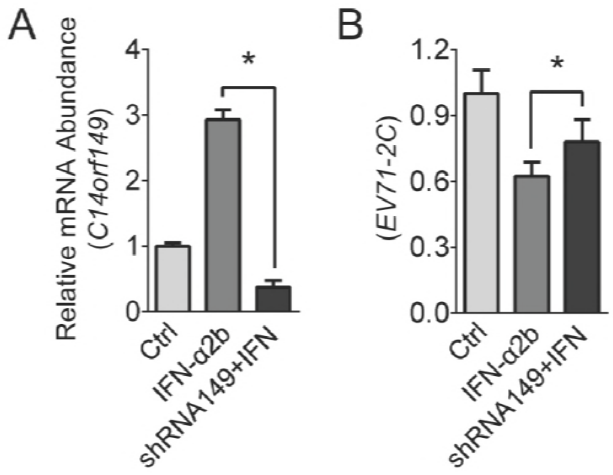

Fig S1. Effects of *L3HYPDH* knockdown on antiviral activity of IFN-α2b against EV71. RT-qPCR analyses of the *L3HYPDH* (A) and EV71 *2C* (B) mRNA in 293A-SCARB2 upon depression of *L3HYPDH* expression by RNAi in the presence of IFN-α2b. 293A-SCARB2 cells were seeded into a 10 cm dish and then transfected with 5 μg of pSUPER-GFP-shRNA149 or pSUPER-GFP. After incubation for 24 h, the GFP-positive cells were isolated using FACS and divided into two parts, one treated with 1000 IU/ml of IFN-α2b, the other mock-treated with water as control, followed by EV71-MZ infection (MOI, 0.1). Eighteen hours post-infection, total RNAs were isolated and used for RT-qPCR measurement. The target mRNA level was normalized to that of GAPDH, and the relative value from the control cells was set as 1. The results are represented as mean±SD of three independent experiments. *, $P<0.05$.